STUDIES OF THE ABILITY TO HOLD THE EYE IN ECCENTRIC GAZE:

Measurements in normal subjects with the head erect

Millard F. Reschke[a]

Jeffrey T. Somers[b]

Alan H. Feiveson[a]

R. John Leigh[c]

Scott J. Wood[d]

William H. Paloski[a]

Ludmila Kornilova[e]

[a]Neurosciences Laboratories, Johnson Space Center. National Aeronautics and Space Administration, Code: SK, Houston, Texas 77058

[b]Wyle Laboratories, Houston, TX 77058

[c]Departments of Neurology, Biomedical Engineering, and Neurosciences
Department of Veterans Affairs Medical Center and University Hospitals,
Case Western Reserve University, Cleveland, Ohio 44106

[d]Universities Space Research Association, Houston TX 77058

[e]Institute of Biomedical Problems, Moscow, Russia

Running title: Gaze-Holding in normals

Acknowledgments: Supported by NSBRI Grant NA00208

Address Correspondence to: Dr. Millard Reschke

NASA Johnson Space Center, 2101 NASA Parkway, Mail Code SK3, Houston, TX 77058

Email: millard.f.reschke@nasa.gov, Phone: 281-483-7210, Fax: 281-244-5734

ABSTRACT

We studied the ability to hold the eyes in eccentric horizontal or vertical gaze angles in 68 normal humans, age range 19-56. Subjects attempted to sustain visual fixation of a briefly flashed target located ±30° in the horizontal plane and ±15° in the vertical plane in a dark environment. Conventionally, the ability to hold eccentric gaze is estimated by fitting centripetal eye drifts by exponential curves and calculating the time constant (τ_c) of these slow phases of "gaze-evoked nystagmus." Although the distribution of time-constant measurements (τ_c) in our normal subjects was extremely skewed due to occasional test runs that exhibited near-perfect stability (large τ_c values), we found that $\log_{10}(\tau_c)$ was approximately normally distributed within classes of target direction. Therefore, statistical estimation and inference on the effect of target direction was performed on values of $z \equiv \log_{10}\tau_c$. Subjects showed considerable variation in their eye-drift performance over repeated trials; nonetheless, statistically significant differences emerged: values of τ_c were significantly higher for gaze elicited to targets in the horizontal plane than for the vertical plane ($P < 10^{-5}$), suggesting eccentric gaze-holding is more stable in the horizontal than in the vertical plane. Furthermore, centrifugal eye drifts were observed in 13.3, 16.0 and 55.6% of cases for horizontal, upgaze and downgaze tests, respectively. Fifth-percentile values of the time constant were estimated to be 10.2 sec, 3.3 sec and 3.8 sec for horizontal, upward and downward gaze, respectively. The difference between horizontal and vertical gaze-holding may be ascribed to separate components of the velocity-to-position neural integrator for eye movements, and to differences in orbital mechanics. Our statistical method for representing the range of normal eccentric gaze stability can be readily applied in a clinical setting to patients who were exposed to environments that may have modified their central integrators and thus require monitoring. Patients with gaze-evoked nystagmus can be flagged by comparing to the above established normative criteria.

KEYWORDS

Gaze-holding, neural integrator, normal population, statistical model, time constant

INTRODUCTION

During natural activities, human subjects often direct their line of sight at an object of interest located off to one side and maintain the eyes at eccentric positions in the orbits while the object is watched. In order to program such "eccentric gaze-holding," the brain must take into account the mechanical properties imposed by the orbital tissues. Specifically, a tonic contraction of the extraocular muscles is necessary to oppose the elastic forces that continually pull back the eye to the central position (Kaneko, 1999, Leigh & Zee, 1999, Robinson, 1974, Seidman, Leigh, Tomsak, Grant & Dell'Osso, 1995). To achieve this sustained muscle contraction, the ocular motoneurons must generate commands with an eye position component. Electrophysiological studies confirm that the ocular motoneurons modulate their discharge rate with eye position (and also with velocity during movements), although the demonstration of orbital pulleys has indicated that the mechanism may be complex (Demer, Miller, Poukens, Vinters & Glasgow, 1995). Premotor neurons that send vestibular (Skavenski & Robinson, 1973), saccadic (Mettens, Godaux, Cheron & Galiana, 1994), and smooth-pursuit signals (Kaneko, 1999) to the ocular motoneurons modulate their discharge with eye velocity, not position. Thus, an integration of velocity-coded premotor signals to position-coded motoneuron commands is achieved by the nervous system. Important components to carry out this integration are: 1) for horizontal gaze-holding, the nucleus prepositus hypoglossi/medial vestibular nuclei complex (NPH/MVN) and 2) for vertical gaze-holding, the interstitial nucleus of Cajal (INC) (Arnold, Robinson & Leigh, 1999, Belknap & McCrea, 1988, Cannon & Robinson, 1987, Helmchen, Rambold, Fuhry & Buttner, 1998, McFarland & Fuchs, 1992). In addition the cerebellum, especially the flocculus, makes an important contribution to the integration (Raymond, Lisberger & Mauk, 1996,

Robinson, 1974, Zee, Leigh & Mathieu-Millaire, 1980). Lesions in any of these structures may impair the ability to hold the eyes in eccentric gaze, allowing the eyes to drift back towards the center of the orbits, causing corrective quick phases, known as "gaze-evoked nystagmus" (Zee, Yamazaki, Butler & Gucer, 1981). Normal subjects also show some centripetal drifts, indicating the neural integrator for eye movements is not perfect, but has a "leak" defined by the time constant of the centripetal drift (τ_c).

In both patients and normal subjects who show gaze-evoked nystagmus, an adaptive mechanism is often evident during sustained efforts to hold the eyes at an eccentric gaze angle. After several seconds, centripetal drift may slow or even reverse in direction, and when the eyes return to central position "rebound nystagmus" results, a transient nystagmus with slow phases directed centrifugally (Bondar, Sharpe & Lewis, 1984, Hood, Kayan & Leech, 1973).

Most prior reports of gaze-holding ability in normals have studied only a few subjects, and have not measured performance in both the horizontal and vertical planes. Thus, the main goal of this study was to establish a normative model of eccentric gaze-holding performance, in both planes, in a healthy subject population, free from vestibular or visual defects. Because of the reported variability of gaze-holding functionality between different subjects (Becker & Klein, 1973, Eizenman, Cheng, Sharpe & Frecker, 1990, Hess, Reisine & Dürstler, 1985, Robinson, Zee, Hain, Holmes & Rosenberg, 1984), we attempted to use a simple methodology that can be easily repeated in both clinical and laboratory settings. Preliminary studies indicated that the distribution of time constant measurements (τ_c) in normal subjects is extremely skewed due to cases that approached perfect stability, ($\tau_c = \infty$). As a result, statistical estimation and inference on the effect of target direction was performed on values of $z \equiv \log_{10}\tau_c$, which we found was well modeled by a normal distribution. Lower percentiles of the estimated normal distributions of z for various modes of testing (horizontal, upward and downward) can be used as standards of

comparison for patients with abnormal gaze-holding ability.

METHODS

Subjects

Horizontal and vertical gaze-holding for eccentric targets were examined in 68 normal subjects (50 males, 18 females, ages 19-56, mean 30.2 years). Testing was performed only after each subject signed a consent form approved by the Johnson Space Center's Institutional Review Board. All subjects were medically screened prior to testing and none presented with vestibular or neurological symptoms, nor were any taking medication with effects on the central nervous system. Subjects were either emmetropes or wore their contact lens corrections during testing.

Equipment

The subjects' eye movements were recorded using either a SensoMotoric Instruments (SMI) EyeLink binocular video eye-tracker (VET) system (linear range of ±30° horizontal and ±20° vertical; sampling rate of 240 Hz; system noise assessed at <0.5° RMS) or an SMI 3-D binocular VET (linear range of ±30° horizontal and ±30° vertical; sampling rate of 60 Hz; system noise assessed at <0.5° RMS) integrated with an in-house pupil tracking algorithm as described previously (Wood, Paloski & Reschke, 1998). The visual stimuli consisted of an array of 5 light-emitting diodes (LEDs), located at center, right and left 30°, and up and down 15°, mounted on a cruciform shaped target, positioned 0.5m from the subject's outer canthus and parallel to the coronal plane. The cruciform target was solidly mounted to a restraint chair in which the subjects were seated. The restraint chair was lightly padded, and included a head and neck restraint that prevented unwanted head movements and assisted the subjects in maintaining straight ahead head and gaze position.

Procedure

All eye movements were obtained in a completely dark environment. Eye movements were calibrated by requiring the subjects to visually acquire a series of LEDs that were displayed in both the horizontal and vertical planes. Following calibration, each trial began with the subject fixating on the center (0°) LED, and then subsequently cued to acquire one of the four eccentric LED targets located at right 30°, left 30°, up 15°, or down 15°. The cue was a transient, 750 milliseconds long flash of the new target LED. Coincident with the 750 milliseconds flash of the eccentric target, the center LED was extinguished. After 20 seconds, the subject was cued with an audio tone to return gaze to the remembered position of the center LED. Gaze was maintained on the remembered central LED position for an additional 20 sec, whereupon the center LED was reilluminated and the subject made any necessary correction in gaze to the central target. The sequence described above was then repeated for a new eccentric target location until all four eccentric targets were displayed.

Data Analysis

The gaze-holding protocol was designed to measure the subject's ability to maintain gaze on a remembered target (first 2 sec of data after acquiring the eccentric target) and to charge the neural integrator for an investigation of rebound nystagmus following a return to center (the remainder of the 20 sec period). Only the first part of the protocol (measurement of gaze-holding) has been analyzed for this paper. The decision to use only the first 2 sec of data for gaze-holding is further justified by the observation that beyond the first 2-3 sec the data were either redundant, gaze had stabilized, or gaze-holding was interrupted by random searching eye movements. Using programs written in MATLAB , the VET signals were filtered using a

median and sliding window filter to remove digitization noise associated with video-oculography (Das, Thomas, Zivotofsky & Leigh, 1996). The data were then calibrated using the initial calibration targets contained at the beginning of each file. To obtain the time constant of centripetal eye drift, each target file was loaded, and the first saccade to the eccentric target was automatically detected and then either accepted for or rejected from analysis interactively. The operator then selected all slow phase drifts within the first two seconds after the initial saccade (Figure 1). We assumed that each drift represented a reset of the neural integrator; therefore, the onset time for each drift was set to zero allowing the fitting algorithm to treat each as the beginning of an exponential curve instead of as a continuation of a previous one. Each drift was then fit using a natural log transformation, converting the data trials with negative positions (*i.e.* left and down trials) to positive values when needed. After applying the natural log transformation to each drift, we performed a linear regression, and used the resultant slope to calculate the time constant ($\tau_c = 1/|\text{ slope }|$) as shown in Figure 2. We excluded individual slow phases with $\tau_c < 1$ sec, since these were more likely to be due to saccadic pulse-step mismatch than due to near-absence of integrator function. All linear regressions with R^2 values below 0.8 were discarded as poor fits. In 23% of drifts, the slow phase drifts moved away from the central position (centrifugally). In these situations, we assumed the drift was moving toward an asymptote located away from center and calculated exponential time constants accordingly. For purposes of assessing gaze-holding ability, we assumed time constants were comparable, regardless of the direction of drift. In other words, a drift in the direction away from center was considered to be as detrimental to clear vision as a similar drift toward center.

Statistical Analysis

After removal of outliers ($\tau_c < 1$), a normal distribution model with random subject

effects was used to describe the distribution of log time-constant measurements for each target direction.

The random-effects model can be expressed by the multilevel model

$$z_{ij} = \mu + a_i + e_{ij} \quad (1)$$

where $z_{ij} = \log_{10}(\tau_c)$ for the *j*-th observation on the *i*-th subject, μ is the mean value of $\log_{10}(\tau_c)$, a_i is a between-subject random effect distributed as N(0, σ_a^2) and e_{ij} is a within-subject error term distributed as N(0, σ^2). All random effects and error terms are assumed statistically independent from each other; however values of the parameters μ, σ_a^2 and σ^2 are allowed to depend on the target direction. From (1), it can be seen that the z_{ij} are distributed marginally as $N(0, \sigma_a^2 + \sigma^2)$, but are not mutually independent as observations pertaining to the same subject (say the *i*-th) have a_i in common. Nevertheless, a histogram of the *z*-values for each target direction can be compared with a best-fitting normal distribution as a corroboration of the model (1) for describing the data. Figure 3 show histograms of z_{ij} with a best-fitting normal distributions for the four target directions, and figure 4 shows the normal probability plots for each of the four target directions. From these figures, it can be seen that the model (1) is excellent for describing this data.

Statistical estimation and inference on the effect of target direction was performed by maximum-likelihood estimation of the statistical parameters in (1) and testing whether μ, σ_a^2 or σ^2 depended on target direction. Because of the monotone log transformation, any significant differences ($P < 0.05$) in the distribution of *z* correspond directly to significant differences in the distribution of τ_c, which follows what is called a "lognormal" distribution. In particular, the median time constant is $\tau_{50} = 10^{\mu}$ and τ_{05}, the 5-th percentile of the marginal distribution of τ_c is equal to $10^{Z_{05}}$ where $Z_{05} = \mu - 1.645(\sigma_a^2 + \sigma^2)^{1/2}$.

The method of iteratively weighted least squares (Goldstein, 1995) was used in MLWIN 1.4 software to do the parameter estimation and the inference. We chose not to use analysis of variance to test for differences in μ between target directions because σ_a^2 or σ^2 could not be assumed invariant with target direction. Furthermore, using MLWIN allowed us to compare σ_a^2 or σ^2 between various target directions. Similar statistical inference could applied on data from clinical studies comparing normal subjects with a group of subjects for which gaze-holding ability is expected to be abnormal.

To obtain a measure of uncertainty in estimates of Z_{05} induced by sampling, we could have used asymptotic standard errors of the model parameter estimates and applied the "delta-method" (Greene, 2000). Instead, we chose to estimate Z_{05} directly, with Bayesian methods using WinBUGS software . The posterior distribution of Z_{05} given the data was then used to construct a "Bayesian credibility interval" analogous to a confidence interval. However, to minimize dependence of our results on assumptions about prior distributions under a Bayesian framework, we used the credibility interval only to obtain an estimate of the ratios of the 5-th and 95-th percentiles of the posterior distribution of Z_{05} to the point estimate (the posterior mean). These ratios were then applied to the standard estimates of Z_{05} from the MLWIN analysis to obtain a 90% confidence interval for Z_{05}. The end points of this confidence interval were then exponentially transformed to obtain a confidence interval for τ_{05}.

RESULTS

Distribution of time-constants

Total sample sizes of 824, 752, 776, and 667 (from 68 subjects) were obtained for the

rightward, leftward, upward, and downward target conditions respectively; however the number of observations per subject varied considerably – from 1 to 93, depending on the target direction. Because of this imbalance, fitting the multilevel model (1) gives a more accurate estimate of population means for each target direction then would simple averaging of the data. For a similar reason, estimates of 5-th percentiles obtained from the multilevel model parameters are more accurate than empirical 5-th percentiles of the data.

First, we fit the model (1) allowing the mean (μ) and both variance components (σ_a^2 and σ^2) of z to vary with target direction. Resulting estimates are shown in Table 1. An examination of this table shows only minor differences in the estimates of the three parameters μ, σ_a and σ^2, between the right and left directions. In addition, in a joint test, these differences were not significantly different from zero ($\chi^2(3) = 3.50$; $P = 0.32$). As a result we combined left and right target data into a single population for subsequent analysis (Table 1, "horizontal"). The most salient feature of Table 1 indicates a substantial decrease in the mean of z (and hence median of τ_c) for vertical relative to horizontal targets, ($\chi^2(1) = 188$; $P < 10^{-5}$) suggesting eccentric gaze-holding is more stable in the horizontal than in the vertical plane. There was also increased variability between subjects for vertical targets ($\chi^2(1) = 23.3$; $P < 10^{-5}$), however the small increase in the within-subject standard deviation for vertical targets was much less clear ($\chi^2(1) = 4.15$; $P = .047$). Although the multilevel parameter estimates appeared to be similar for the up and down target directions, the hypothesis of overall equality of μ, σ_u and σ was rejected ($\chi^2(3) = 10.01$; $P = 0.018$). Furthermore, we observed that 43% of drifts elicited to downward targets were away from center (centrifugal) compared to only 22% of drifts associated with upward targets. Therefore we felt there was, at a minimum, a functional difference between upward and downward vertical gaze and we suggest using distinct 5-th percentile values for these cases.

Table 1 also shows the estimates of the median (τ_{50}) and 5-th percentile (τ_{05}) of the time-constant distribution, as well as the lower and upper confidence limits for the 5-th percentile (τ_{05}) (*Statistical Analysis*).

Applying the Model

For the horizontal, upward, and downward target directions, histograms of time constants are shown in Figure 5, with superimposed best-fitting lognormal distributions, using the parameter values in Table 1. Because there was no statistical difference between gaze-holding to rightward and leftward targets, the horizontal data were pooled and a single lognormal distribution was fit to the data. On each panel, estimated 5-th percentiles of these distributions are indicated by vertical lines. Of particular interest is difference between horizontal and vertical time constants apparent in the abscissa scales of each pane. In a clinical setting, one would simply apply the appropriate 5-th percentile from Table 1 as a threshold to flag potentially abnormal gaze-holding performance. The probability of being able to detect a particular pathology by this method would depend on how much the time-constant distribution is shifted (presumably downwards). To illustrate this point, figure 6 indicates how well these thresholds would be able to successfully detect abnormalities (up and down results were averaged for this plot because their difference was relatively small). The figure depicts the probability of the subject's time constant distribution would fall below the 5-th percentile threshold value given in Table 1. For a zero percent change in median time constant (no shift in the subject's distribution relative to the distribution of normal subjects), the probability of a singe drift falling below the threshold would be 0.05 as expected. As an example, if the median time constant were to shift by 50%, however, the probability of a single drift falling below the threshold would now be 0.26 for horizontal and 0.21 for vertical.

DISCUSSION

We set out to compare the ability to hold steady eccentric gaze in the horizontal versus vertical planes in a large group of healthy human subjects. There are two main findings of this study. First, using a logarithmic transformation of the time constant of drift is a reasonable approach to dealing with extremely skewed time-constant data. This approach provides a means to summarize the normal range and define abnormal gaze-holding ability. Second, using this statistical approach, we have been able to show that normal subjects show better eccentric gaze-holding ability in the horizontal than the vertical plane.

Development of a New Statistic for Measurement of Gaze-holding

Normal subjects are able to hold gaze well in darkness, leading to a highly skewed distribution of time constants (containing extremely large values). As a result, it is more mathematically expedient to model the distribution of logarithmic transformation of the time constants than the time constants directly. We estimated the distributions using a normal distribution and found this to be a reasonable approach and provides a means to summarize the normal range and define abnormal gaze-holding ability.

It should be noted that our estimates of the time constant are based on eye drifts when subjects attempted to view a remembered target located at ±30° in the horizontal plane and ±15° in the vertical plane. Although it is convenient to assume a linear model for the ocular motor plant and an integrator with a single time constant, in practice this is not observed. Thus, it is known that with greater eccentricity, different time constants are observed, (Abel, Dell'osso & Daroff, 1978) for which a neural mechanism has been proposed (Cannon & Robinson, 1985). Application of our statistical results depends on similar target locations being used during testing. How well the normal distribution could fit data generated during attempts to fixate targets at the extremes of gaze requires further study. Nonetheless, the eccentricities that we have

chosen are those which challenge gaze-holding ability, but are within the linear range of most eye movement monitors.

Possible Physiological and Anatomical Basis for Current Findings

A number of prior studies (Abel, S. & Dell'Osso, 1983, Becker & Klein, 1973, Eizenman et al., 1990, Robinson et al., 1984) have reported that normal subjects show a range of ability (measured by time-constant of centripetal eye drift) to hold steady horizontal eccentric gaze in darkness. Indeed, some normal subjects show "end-point nystagmus" when viewing a target (Abel, Parker, Daroff & Dell'Osso, 1978). In the present study of normal subjects, we show that the range of normal gaze-holding ability in the horizontal plane is less stable than previously reported, and for the first time, have demonstrated that eccentric vertical gaze holding is also less stable than horizontal gaze holding. One possible explanation for the difference in horizontal and vertical relates to the observation that different structures of the brainstem, and perhaps the cerebellum, contribute to horizontal or vertical gaze-holding in monkeys. For example, chemical lesions of NPH/MVN in the medulla abolish horizontal gaze-holding ability, but leave some gaze-holding ability intact (Cannon & Robinson, 1987). On the other hand, pharmacological inactivation of INC in the midbrain mainly impairs vertical gaze-holding ability (Crawford, 1994, Crawford, Cadera & Vilis, 1991). Another contributing factor concerns the mechanical properties of the orbital tissues. The discovery of pulleys that guide the extraocular muscles might provide an explanation based on orbital mechanics. Thus, each extraocular muscle comprises an outer orbital layer that attaches to a pulley (and moves it), and an inner global layer that passes through the pulley and inserts onto the eyeball. For example, Demer (Demer, 2003) has suggested that the restricted range of upward gaze movement encountered in normal elderly subjects may be due to changes in the attachment of the orbital layer of the inferior oblique muscle to other connective tissues in the orbit. The subjects that we studied were predominantly

young and showed no limitation of upward gaze. Although there was no asymmetry of upward versus downward time constant, we did note a larger percentage of drifts away from center when looking to the downward target. Future studies of older healthy populations might show significant differences.

ACKNOWLEDGEMENTS

This work supported by the National Space Biomedical Research Institute through NASA NCC 9-58 (Grant NA00208).

REFERENCES

(1996-2004). WinBUGS. (Cambridge, UK: Imperial College and Meidcal Research Council.

(2002a). MATLAB. (Natick, MA: The Mathworks.

(2002b). MLwiN. (London, UK: Centre for Multilevel Modelling team.

Abel, L.A., Dell'osso, L.F., & Daroff, R.B. (1978). Analog model for gaze-evoked nystagmus. *IEEE Trans Biomed Eng, 25* (1), 71-75.

Abel, L.A., Parker, L., Daroff, R.B., & Dell'Osso, L.F. (1978). End-point nystagmus. *Invest Ophthalmol Vis Sci, 17* (6), 539-544.

Abel, L.A., S., T., & Dell'Osso, L.F. (1983). Variable waveforms in downbeat nystagmus imply short-term gain changes. *Ann Neurol, 13*, 616-620.

Arnold, D.B., Robinson, D.A., & Leigh, R.J. (1999). Nystagmus induced by pharmacological inactivation of the brainstem ocular motor integrator in monkey. *Vision Res, 39* (25), 4286-4295.

Becker, W., & Klein, H.M. (1973). Accuracy of saccadic eye movements and maintenance of eccentric eye positions in the dark. *Vision Res, 13* (6), 1021-1034.

Belknap, D.B., & McCrea, R.A. (1988). Anatomical connections of the prepositus and abducens nuclei in the squirrel monkey. *J Comp Neurol, 268* (1), 13-28.

Bondar, R.L., Sharpe, J.A., & Lewis, A.J. (1984). Rebound nystagmus in olivocerebellar atrophy: a clinicopathological correlation. *Ann Neurol, 15* (5), 474-477.

Cannon, S.C., & Robinson, D.A. (1985). An improved neural-network model for the neural integrator of the oculomotor system: more realistic neuron behavior. *Biol Cybern, 53* (2), 93-108.

Cannon, S.C., & Robinson, D.A. (1987). Loss of the neural integrator of the oculomotor system

from brain stem lesions in monkey. *J Neurophysiol, 57* (5), 1383-1409.

Crawford, J.D. (1994). The oculomotor neural integrator uses a behavior-related coordinate system. *J Neurosci, 14* (11 Pt 2), 6911-6923.

Crawford, J.D., Cadera, W., & Vilis, T. (1991). Generation of torsional and vertical eye position signals by the interstitial nucleus of Cajal. *Science, 252* (5012), 1551-1553.

Das, V.E., Thomas, C.W., Zivotofsky, A.Z., & Leigh, R.J. (1996). Measuring eye movements during locomotion: filtering techniques for obtaining velocity signals from a video-based eye monitor. *J Vestib Res, 6* (6), 455-461.

Demer, J. (2003). Ocular kinematics, vergence, and orbital mechanics. *Strabismus, 11* (1), 49-57.

Demer, J.L., Miller, J.M., Poukens, V., Vinters, H.V., & Glasgow, B.J. (1995). Evidence for fibromuscular pulleys of the recti extraocular muscles. *Invest Ophthalmol Vis Sci, 36* (6), 1125-1136.

Eizenman, M., Cheng, P., Sharpe, J.A., & Frecker, R.C. (1990). End-point nystagmus and ocular drift: an experimental and theoretical study. *Vision Res, 30* (6), 863-877.

Goldstein, H. (1995). Multilevel Statistical Models. (London, UK: Edward Arnold Press.

Greene, W.H. (2000). Econometric Analysis. (Upper Saddle River, NJ: Prentice Hall.

Helmchen, C., Rambold, H., Fuhry, L., & Buttner, U. (1998). Deficits in vertical and torsional eye movements after uni- and bilateral muscimol inactivation of the interstitial nucleus of Cajal of the alert monkey. *Exp Brain Res, 119* (4), 436-452.

Hess, W., Reisine, H., & Dürstler, M.R. (1985). Normal eye drift and saccadic drift correction in darkness. *Neuro-ophthalmology, 5*, 247-252.

Hood, J.D., Kayan, A., & Leech, J. (1973). Rebound nystagmus. *Brain, 96* (3), 507-526.

Kaneko, C.R. (1999). Eye movement deficits following ibotenic acid lesions of the nucleus prepositus hypoglossi in monkeys II. Pursuit, vestibular, and optokinetic responses. *J*

Neurophysiol, 81 (2), 668-681.

Leigh, R.J., & Zee, D.S. (1999). The neurology of eye movements. *Contemporary neurology series ; 55.* (pp. x, 643). New York: Oxford University Press.

McFarland, J.L., & Fuchs, A.F. (1992). Discharge patterns in nucleus prepositus hypoglossi and adjacent medial vestibular nucleus during horizontal eye movement in behaving macaques. *J Neurophysiol, 68* (1), 319-332.

Mettens, P., Godaux, E., Cheron, G., & Galiana, H.L. (1994). Effect of muscimol microinjections into the prepositus hypoglossi and the medial vestibular nuclei on cat eye movements. *J Neurophysiol, 72* (2), 785-802.

Raymond, J.L., Lisberger, S.G., & Mauk, M.D. (1996). The cerebellum: a neuronal learning machine? *Science, 272* (5265), 1126-1131.

Robinson, D.A. (1974). The effect of cerebellectomy on the cat's bestibulo-ocular integrator. *Brain Res, 71* (2-3), 195-207.

Robinson, D.A., Zee, D.S., Hain, T.C., Holmes, A., & Rosenberg, L.F. (1984). Alexander's law: its behavior and origin in the human vestibulo-ocular reflex. *Ann Neurol, 16* (6), 714-722.

Seidman, S.H., Leigh, R.J., Tomsak, R.L., Grant, M.P., & Dell'Osso, L.F. (1995). Dynamic properties of the human vestibulo-ocular reflex during head rotations in roll. *Vision Res, 35* (5), 679-689.

Skavenski, A.A., & Robinson, D.A. (1973). Role of abducens neurons in vestibuloocular reflex. *J Neurophysiol, 36* (4), 724-738.

Wood, S.J., Paloski, W.H., & Reschke, M.F. (1998). Spatial coding of eye movements relative to perceived earth and head orientations during static roll tilt. *Exp Brain Res, 121* (1), 51-58.

Zee, D.S., Leigh, R.J., & Mathieu-Millaire, F. (1980). Cerebellar control of ocular gaze stability. *Ann Neurol, 7* (1), 37-40.

Zee, D.S., Yamazaki, A., Butler, P.H., & Gucer, G. (1981). Effects of ablation of flocculus and paraflocculus of eye movements in primate. *J Neurophysiol, 46* (4), 878-899.

Table 1. Parameter estimates by target direction

target direction	μ	σ_u	σ_e	τ_{50}	τ_{05}	τ_{05} lower	τ_{05} upper
right	1.48	0.18	0.25	30.3	9.6	8.9	11.4
left	1.53	0.16	0.26	33.7	10.7	9.0	11.3
horizontal	1.51	0.17	0.25	32.0	10.2	9.0	11.3
up	1.10	0.22	0.27	12.6	3.3	2.85	3.83
down	1.18	0.20	0.30	15.0	3.8	3.24	4.31

Figure Legends

Figure 1: Representative gaze-holding trial. The subject begins by fixating the center LED and then makes a saccade to a left 30° target. The subject maintains the approximate gaze angle for 20 seconds before being cued to return to center by and audio tone. After 20 seconds at center, the center LED is reilluminated. INSERT: During analysis, the drifts from the first 2 seconds after the first saccade are selected interactively (highlighted sections).

Figure 2: Natural log transformation and linear regression. Using the same data as in Figure 1, each drift was inverted and reset to a start time of zero. The natural log was applied and then a linear regression was used to fit the data. The equations of the fit are shown as well as the time constants. Note the variability within one subject's trial.

Figure 3: Empirical log-transformation distributions and associated normal models. Shown are target data histograms and models for all 68 subjects for (A) rightward, (B) leftward, (C) upward, and (D) downward target directions. Note each 5^{th} percentile point (denoted by a vertical line) and the associated values (1.03, 0.98, 0.51, and 0.59 $\log_{10}$ sec respectively).

Figure 4: Normal probability plots. Shown are the normal probability plots for all 68 subjects for (A) rightward, (B) leftward, (C) upward, and (D) downward target directions. Note that for each target direction, the data are well described as normal (linear trend).

Figure 5: Time constant distributions and lognormal model. Shown are time constant histograms and approximated lognormal models for all 68 subjects for (A) horizontal, (B) upward, and (C) downward target directions. Note each 5^{th} percentile point (denoted by a vertical line) and the associated values (10.2, 3.3, and 3.8 sec respectively). These points can serve as

estimates for the difference between normal and abnormal gaze-holding response to similar target locations. Note the vertical target time constant scales (panels B & C) are half the scale of the horizontal distribution (panel A). Also, note the similarity between the upward and downward gaze-holding distributions and models.

Figure 6: Detection probability plot. Shown is the probability of a single drift being identified as abnormal (below the normative 5th percentile) based on the percent drop in median time constant. Note that for a 0% drop in time constant (no change), the probability is 5% meaning that any particular drift would have a 0.05 probability of 0.05 as being identified as abnormal. If the median time constant for a subject were shifted by 50% from normal, we would expect a single drift to have a probability of 0.26 as being identified as being abnormal for horizontal targets and 0.21 for vertical targets.

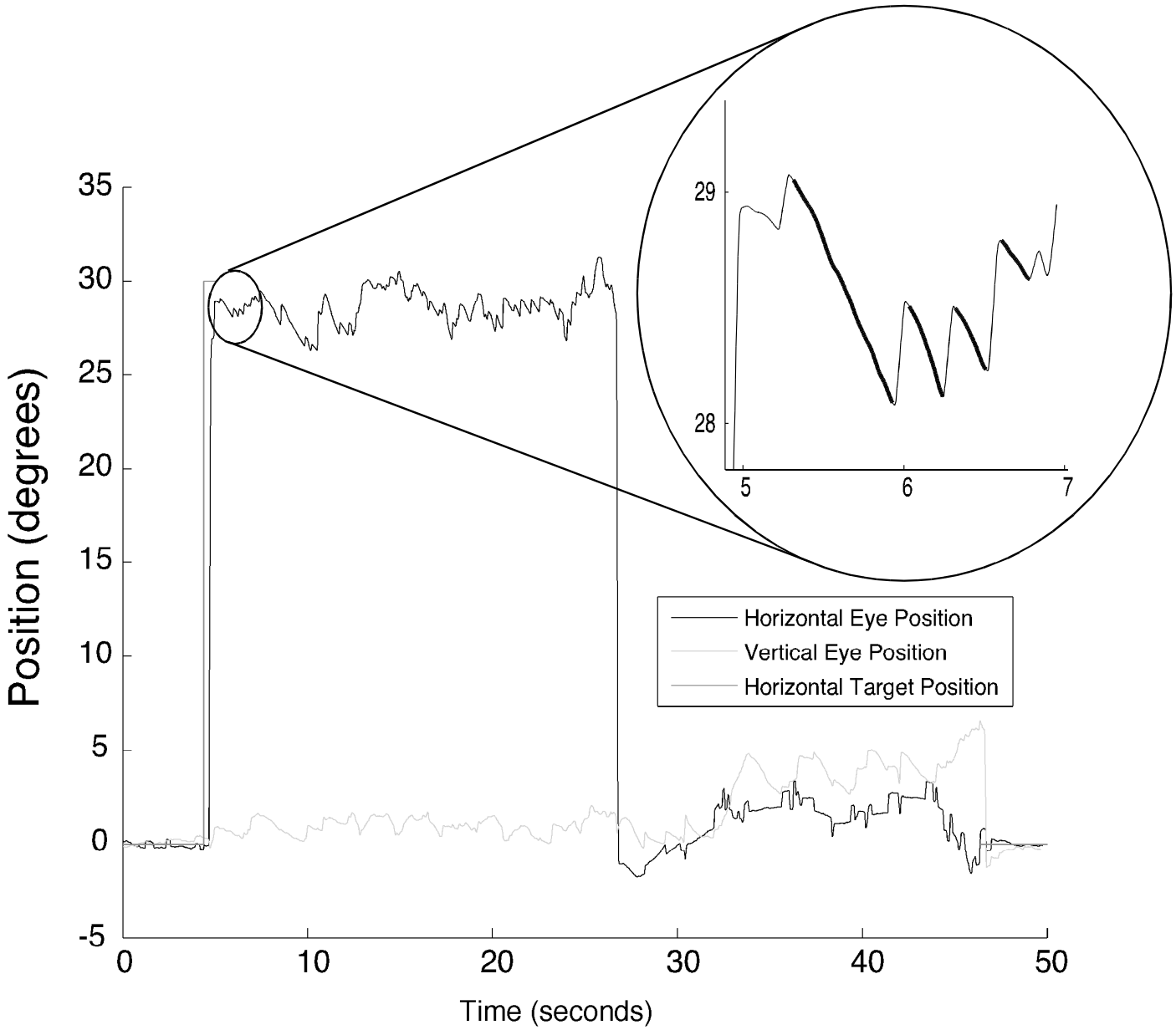
Position (degrees)
35
30
25
20
15
10
5
0
-5
0
10
20
30
40
50
Time (seconds)
29
28
5
6
7
Horizontal Eye Position
Vertical Eye Position
Horizontal Target Position

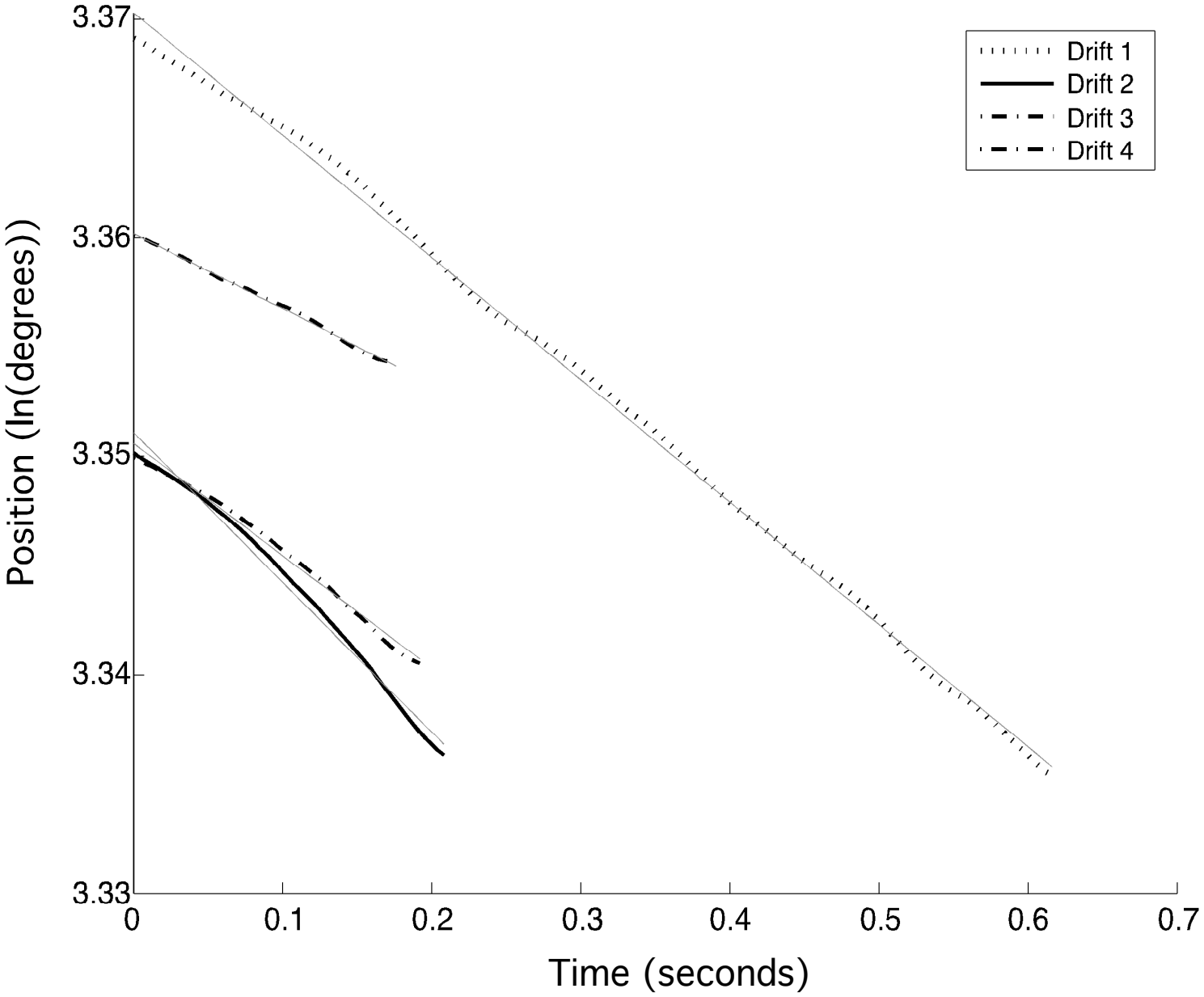
Drift 1
Drift 2
Drift 3
Drift 4
Position (ln(degrees))
Time (seconds)
3.37
3.36
3.35
3.34
3.33
0
0.1
0.2
0.3
0.4
0.5
0.6
0.7

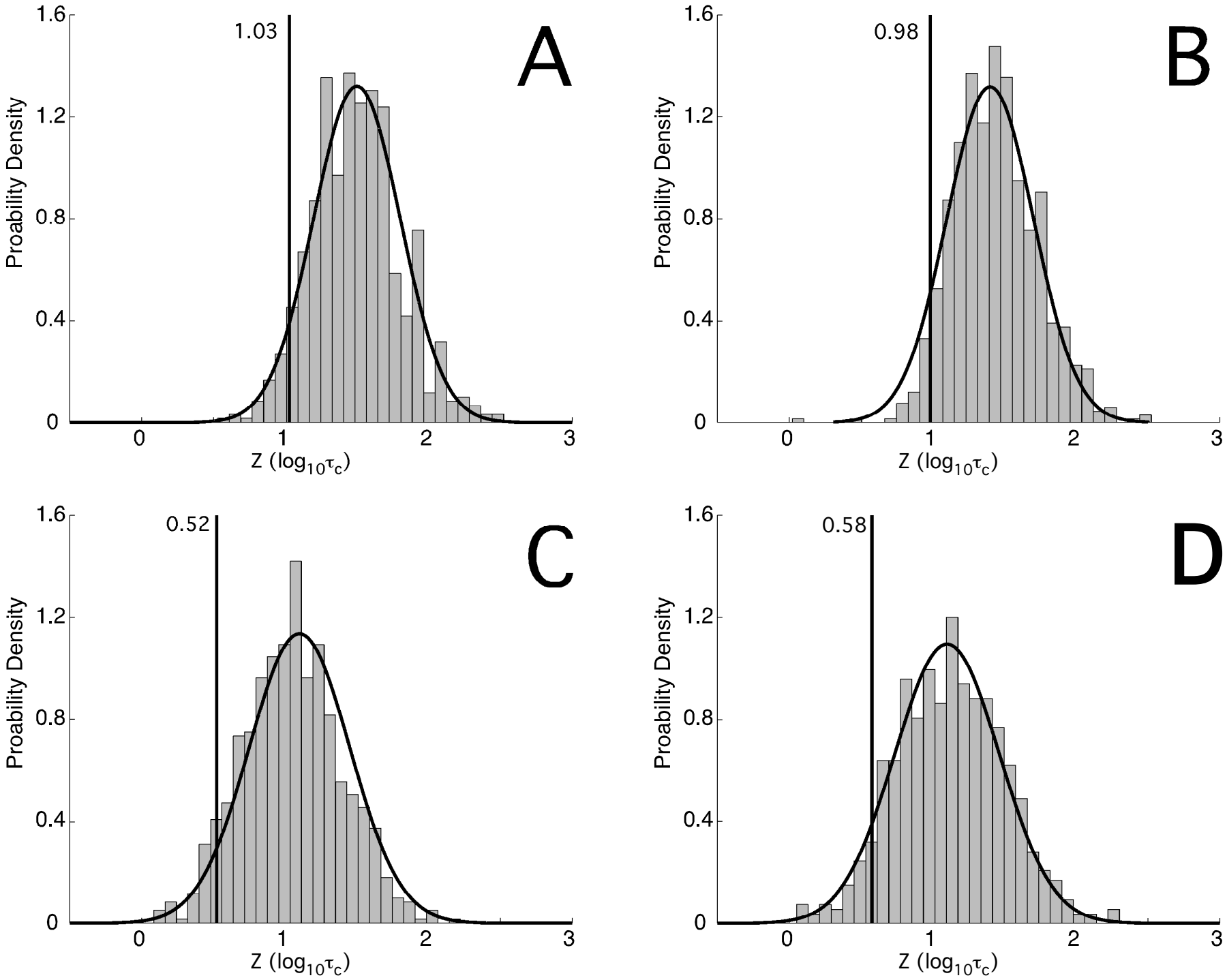
A
1.03
Proability Density
Z ($\log_{10}\tau_c$)
B
0.98
Proability Density
Z ($\log_{10}\tau_c$)
C
0.52
Proability Density
Z ($\log_{10}\tau_c$)
D
0.58
Proability Density
Z ($\log_{10}\tau_c$)

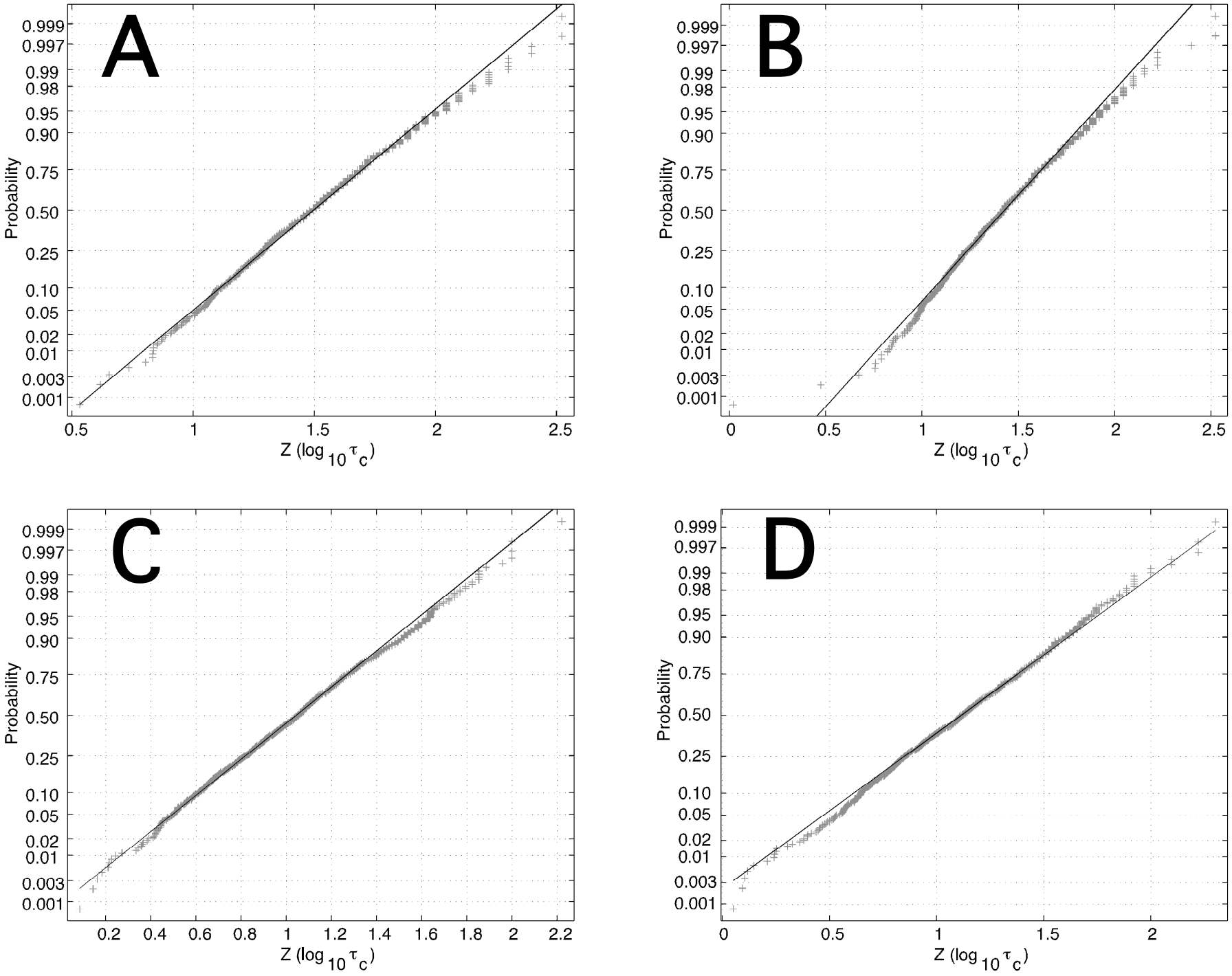
A
B
C
D
Probability
0.999
0.997
0.99
0.98
0.95
0.90
0.75
0.50
0.25
0.10
0.05
0.02
0.01
0.003
0.001
Z (log 10 τc)
0.5
1
1.5
2
2.5
0
0.2
0.4
0.6
0.8
1.2
1.4
1.6
1.8
2.2

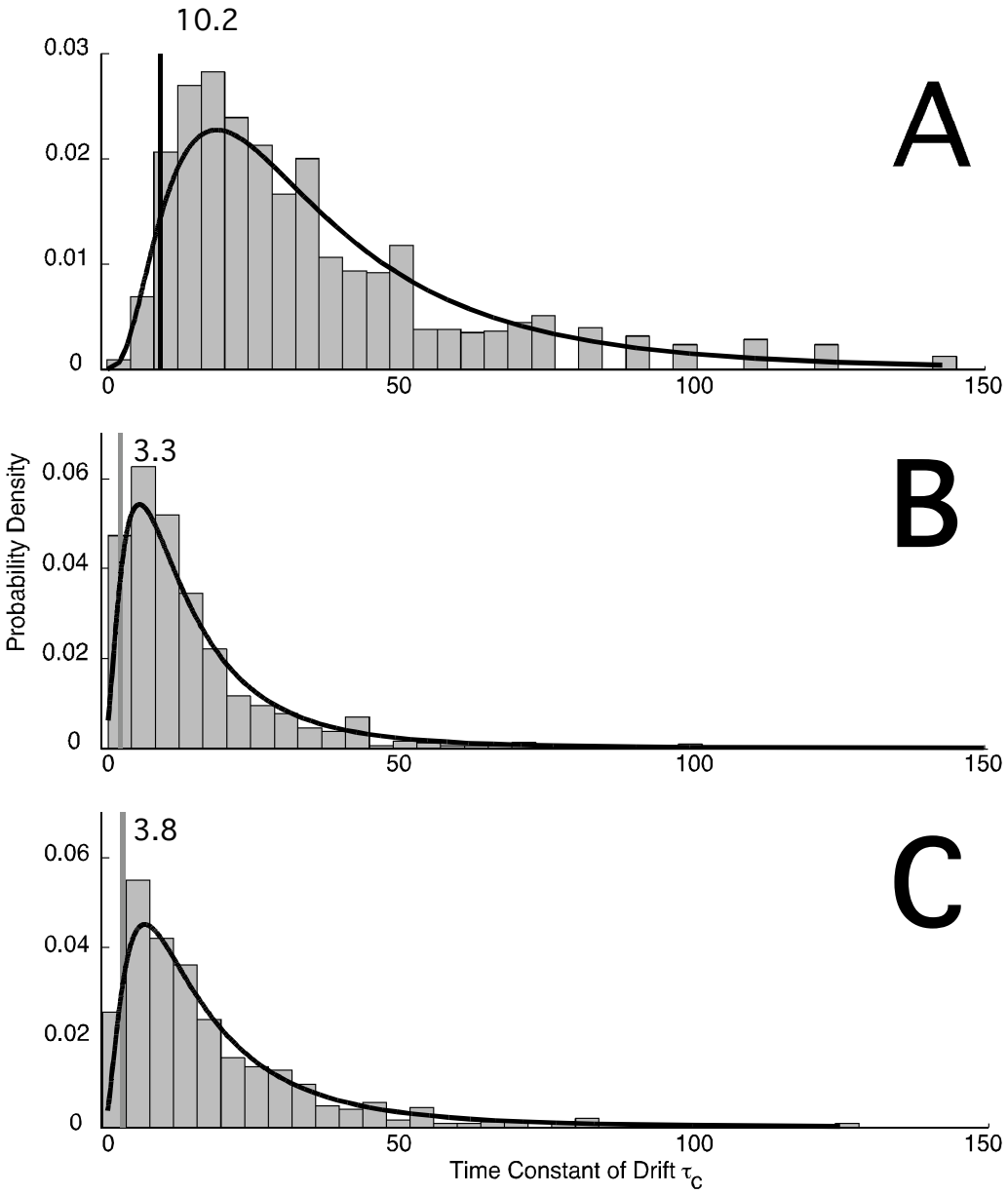
10.2
A
3.3
B
3.8
C
Probability Density
0.03
0.02
0.01
0
0.06
0.04
0.02
0
0
50
100
150
Time Constant of Drift τ_c

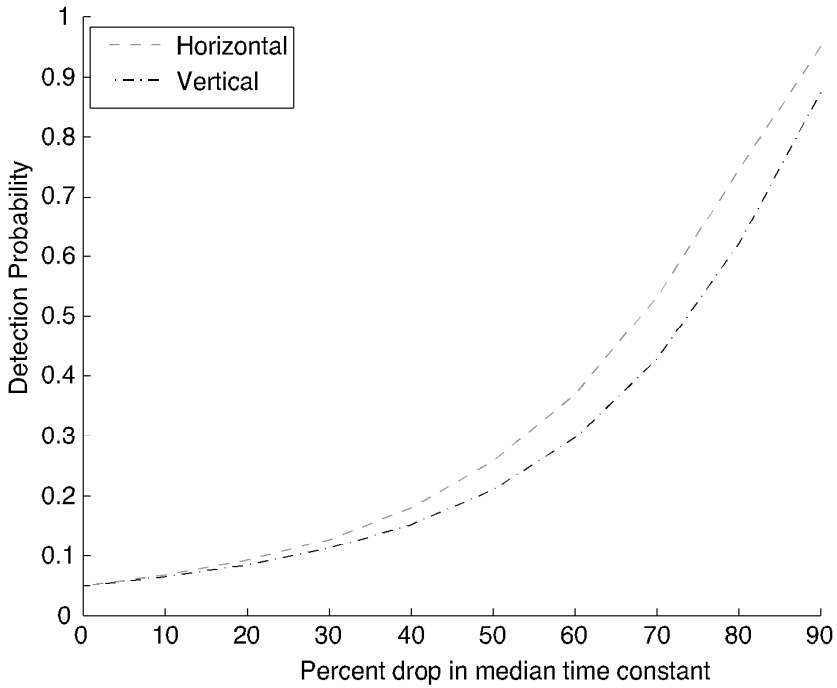
Horizontal
Vertical
Detection Probability
Percent drop in median time constant
0
0.1
0.2
0.3
0.4
0.5
0.6
0.7
0.8
0.9
1
0
10
20
30
40
50
60
70
80
90